Statistical Analysis of Sea Clutter at Low Grazing Angle

Zhou Peng[1, a], Xie Hongsen[1, a], Wang Ding[1, b], Tian Huaming[1, b]

Naval Aeronautical Engineering Academy, QingDao, ShanDong, 266041

[a]email: qdrfeng@sohu.com, [b]email:825834868@qq.com

Keywords: sea clutter, non-Gaussian, non-stationarity, non-homogeneity, statistical characteristics.

Abstract. A lot of literatures indicate that, the statistical characteristics of sea clutter at low grazing angle can be modeled as compound Gaussian process, which is the product of speckle with shorter coherent length and texture with longer coherent length, and is non-Gaussian, non-homogeneous, and non-stationary. In this paper, for the X-band sea clutter, with different range resolutions and polarization, the extraction algorithm of texture is given, and power spectrum density of clutter is analyzed at first. The results show that the power spectrum density of clutter can be modeled as exponential model. Secondly, the non-Gaussian of clutter is analyzed in temporal and spatial domain, and the results show that the amplitude probability density function can be fit to the generalized K distribution with Log-Normal texture. The non-stationarity and non-homogeneity of sea clutter is analyzed at last.

Introduction

The sea clutter is generated by the backscattering of the electromagnetic waves from the sea level. The statistical characteristics of the clutter are closely related to the fluctuation of sea level, the meteorological conditions and the working parameters of radar [1]. When the grazing angle is less than 10 degrees, the high resolution radar's sea clutter statistical wave characteristics will significantly deviate from the Gaussian distribution, and the statistical nature of its amplitude will have a "fat tail" effect, i.e. the probability of large amplitude clutter's appearance to increases. The clutter's amplitude shows more spikes. Doppler power spectrum characteristics of sea clutter is related to wave structure, wind speed and direction, and the statistical characteristics of sea clutter changes over time and space, showing the non-stationarity and non-homogeneity.

In the problem of radar signal detection, the conventional detection algorithm is aimed at the clutter of the Gauss distribution, and its performance will be significantly decreased when it is applied to the non Gauss clutter[2]. In order to estimate the clutter correlation function of the waiting detection unit, the clutter data of the nearby range unit is usually estimated[3]. The non-stationarity and non-homogeneity of the clutter statistics has seriously affected the estimation of the clutter correlation function of the waiting detection unit. For the signal detection problem in non-Gaussian and non-stationary and non-homogeneous clutter environment, in this paper, the non-Gauss, non-stationarity and non-homogeneity of the sea clutter of low grazing angle at different resolution and different polarization are analyzed[1]-[4], and the results of the analysis contribute to the design and analysis of signal detection algorithm performance in sea clutter environment, and improving the signal detection capability.

In this paper, the radar clutter data obtained from IPIX radar of McMaster University in Canada in 1998 is analyzed. The specific parameters of the clutter are also found in literature [5]. And the results of [5] show that, the radar clutter data can fit the SIRV model well in most cases. Based on this, the non - Gauss, non-stationarity and non-homogeneity of radar clutter is further analyzed.

Extracting the texture component of sea clutter

The texture component of sea clutter is extracted essentially based on that texture component and speckle component have different coherence lengths. In literature [6], the algorithm of calculating the coherence length of the texture components of the sea clutter is given, and the algorithm is based on the generalized Kolmogorov-Smirnov test. In this paper, a new texture component extraction algorithm is proposed, which can adaptively search the optimal texture component coherence length without statistical hypothesis testing. Assuming the length of clutter texture component is L, then the noise sequence of length L can be approximated as:

$$\begin{aligned}\mathbf{c} &= \left\{c\left(k-L/2+1\right),...,c\left(k\right),c\left(k+1\right),...,c\left(k+L/2\right)\right\} \\ &\approx \left\{\sqrt{\tau\left(k\right)}g\left(k-L/2+1\right),...,\sqrt{\tau\left(k\right)}g\left(k\right),\sqrt{\tau\left(k\right)}g\left(k+1\right),...,\sqrt{\tau\left(k\right)}g\left(k+L/2\right)\right\}\end{aligned} \tag{1}$$

Without loss of generality, It can be assumed that the speckle component is a Gauss distribution of the zero mean unit variance, then the speckle components of the serial number k can be estimated:

$$\hat{g}\left(k\right)=\frac{c\left(k\right)}{\sqrt{\sum_{l=-L/2+1}^{L/2}\left|c\left(k+l\right)\right|^2}} \tag{2}$$

So the fitting degree of speckle estimation and Gauss distribution can be used as the estimation effect of texture component coherence length:

$$\hat{L}=\min_{L} d\left(L\right)=\min_{L}\int\left|\hat{f}\left(g\right)-f\left(g\right)\right|^2 \mathrm{d}g \tag{3}$$

Among that, $\hat{f}\left(\cdot\right)$ is the empirical PDF of speckle component estimation, and $f\left(\cdot\right)$ is the PDF of Gauss distribution, and mean and variance are derived from the valuation of speckle components. Then the fitting degree of the two PDF is obviously related to the coherence length L of texture component. When the coherence length L of texture components is close to the true value, the speckle component is close to the Gauss distribution, and the minimum value of $d\left(L\right)$ is reached. But when the coherence length L of texture components deviates from the true value, whether it is smaller or larger, the value of $d\left(L\right)$ will increase, so $d\left(L\right)$ should be a convex function, and have only one minimum. Therefore, by use of this property of $d\left(L\right)$, the valuation of L corresponding to the minimum value of the function $d\left(L\right)$ can be obtained through the simplest search algorithm in actual estimation process.

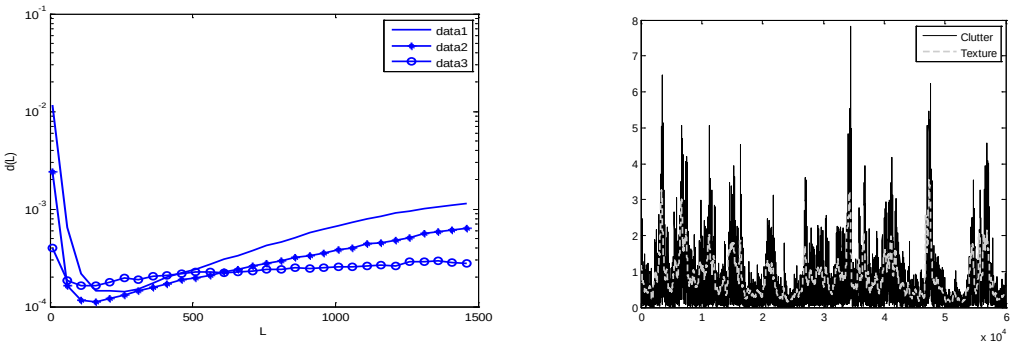

(a) Different clutter data in HH mode $d\left(L\right)$ (b) Texture extraction of clutter data Data1

Figure 1. Texture component extraction algorithm

Figure 1 shows the process and results of texture extraction algorithm. Figure 1 (a) shows the curve of $d\left(L\right)$ in HH mode in three resolutions, obviously, $d\left(L\right)$ is approximated as a curve

lower convex which has a single minimum, and its minimum value corresponds to the best estimate of the texture component coherence length. It should be noted that, Even if $d(L)$ reaches a minimum, the size of the minimum is related to the choice of the data. Among them, data3 has a higher resolution, and the minimum of $d(L)$ is larger than that of other data. This shows that, the speckle component of the data fits Gauss worst. The conclusion of [6] shows that the fitting degree of the data and SIRV is the worst. In Fig. 1 (b), in view of the clutter Data1 in HH mode, the effect of the extraction of texture component is given, which basically reflects the change of the average power of the clutter.

Table 1. Coherence length of radar clutter

	HH	HV	VH	VV
Data1	272	146	246	171
Data2	146	121	296	171
Data3	109	96	21	21

Table 1 gives the coherence length of the texture components of the radar clutter data with the distance element number 17. It can be found that the HH polarization has a longer texture component coherence length, while the VV polarization is usually smaller. Secondly, the coherence length of the texture component decreases with increasing resolution. In radar signal detection, when the coherent processing pulse number is more than the coherence length of the texture component, the SIRV model of clutter is no longer valid, and degenerates into the compound Gauss model, so many of the assumptions based on the SIRV signal detection algorithm are no longer valid. That is to say, for sea clutter, detection performance could not be always improved by increasing the number of coherent pulse.

Average power spectrum analysis of sea clutter

The power spectral model is usually used in the position - scale model, and the model has two main parameters, which correspond to the center and the width of the power spectrum. The four power spectrum models are considered in this paper.

Exponential model (Expo):

$$S(f)=\exp\left(-\alpha\left|f-f_0\right|\right) \tag{4}$$

Gauss model (Gauss):

$$S(f)=\exp\left(-\alpha\left|f-f_0\right|^2\right) \tag{5}$$

First order power-law model (PL-1):

$$S(f)=\frac{1}{1+\alpha\left|f-f_0\right|} \tag{6}$$

Two order power-law model (PL-2):

$$S(f)=\frac{1}{1+\alpha\left|f-f_0\right|^2} \tag{7}$$

By using the nonparametric spectrum estimation method (the Welch spectrum estimation method), the length selection 1024, and the 50% overlapping, the power spectrum estimation of the clutter ($\hat{S}(f)$) is obtained, and the parameters of the power spectrum model are as follows:

$$\left(\hat{\alpha},\hat{f}_0\right)=\min_{\alpha,f}J(\alpha,f_0)=\min_{\alpha,f}\int\left|\hat{S}(f)-S(f;\alpha,f_0)\right|^2\mathrm{d}f \tag{8}$$

Using the nonlinear least square method, the parameter estimation of different power spectrum

models can be obtained. Then the optimal model of the above power spectrum model can be determined according to the size of $J(\alpha, f_0)$.

Table 2. Power Spectrum model fitting error (10^{-4})

	PSD Model	HH	HV	VH	VV
Data1	Expo	**22.8505**	**18.2165**	**17.8111**	**32.5545**
	Gaus	35.7506	42.7133	42.2131	46.6254
	PL-1	74.4459	62.4505	62.1469	93.5759
	PL-2	27.6709	26.3523	25.8588	43.4418
Data2	Expo	**19.6286**	**25.9079**	**25.8537**	**31.3215**
	Gaus	57.1443	56.9694	58.4566	49.1438
	PL-1	30.6062	41.9932	44.6901	78.5305
	PL-2	32.7676	37.8385	38.7891	43.1234
Data3	Expo	25.9183	50.8908	42.6557	**29.6251**
	Gaus	42.2044	89.3719	83.2424	58.0731
	PL-1	**16.8867**	**40.3196**	**32.2053**	38.3496
	PL-2	28.4516	63.6718	56.6132	42.3321

Table 2 gives the error results of the power spectrum fitting of the distance element number 17. It can be seen from the table that, the power spectral exponential model of Data2 and Data1 is appropriate. However, for Data3, except for the VV polarization mode, the exponential model is better in other polarization modes. Corresponding to the optimum power spectrum model, the best fitting parameters can be obtained, and the center frequency and 3dB bandwidth of the power spectrum can also be obtained easily.

Non-Gaussian analysis of sea clutter

Statistical analysis of amplitude of sea clutter.

The study of the Non-Gaussian of sea clutter is also discussed in the literature [5], but it only discusses the distribution of Rayleigh, Weibull and K. And this paper further expands the generalized K distribution (GK-LNT) with the log normal distribution (LN), generalized K distribution (GK) and generalized K distribution based on log normal distribution texture (GK-LNT) [7]. The model of the amplitude distribution of the above clutter and its N moments are summarized as follows.

(1) Lognormal distribution model (LN):

$$p_X(x \mid \mu, \sigma) = \frac{1}{x\sqrt{2\pi\sigma^2}} \exp\left(-\frac{1}{2\sigma^2}\ln^2\left(\frac{x}{\mu}\right)\right); x \geq 0 \tag{9}$$

$$E\left[x^n\right] = \mu^n \exp\left(\frac{n^2\sigma^2}{2}\right) \tag{10}$$

Among them, μ is the Scale parameter, σ is Shape parameter.

(2) Generalized K distribution model (GK)

$$p(x \mid \mu, \nu, b) = \frac{2bx}{\Gamma(\nu)}\left(\frac{\nu}{\mu}\right)^{\nu b} \int_0^\infty \tau^{\nu b-2} \exp\left(-\frac{x^2}{\tau} - \left(\frac{\nu}{\mu}\tau\right)^b\right) d\tau \tag{11}$$

$$E\left[x^n\right] = \left(\frac{\mu}{\nu}\right)^{n/2} \frac{\Gamma(\nu + n/2b)\Gamma(1+n/2)}{\Gamma(\nu)} \tag{12}$$

K distribution is the special case of GK distribution (b=1).

(3)GK-LNT distribution model

$$p(x \mid \sigma, \delta) = \frac{x}{\sqrt{2\pi\sigma^2}} \int_0^\infty \frac{2}{\tau^2} \exp\left(-\frac{x^2}{\tau} - \frac{1}{2\sigma^2}\ln^2\left(\frac{\tau}{\delta}\right)\right) d\tau \tag{13}$$

$$E\left[x^n\right] = (\delta)^{n/2}\Gamma(1+n/2)\exp\left(\frac{1}{2}\left(\frac{n\sigma}{2}\right)^2\right) \tag{14}$$

The parameters of above amplitude distribution models can be obtained by moment matching method. Among them, parameters of Rayleigh distribution, lognormal distribution and GK-LNT distribution can be estimated by the one or two order moments of the clutter data directly. But the parameters of Weibull distribution, K distribution need to be solved by numerical approximation through nonlinear equations. For the generalized K distribution, in order to obtain the parameters, a multi moment estimation is needed. In this paper, the parameters are estimated by use of 2 ~ 6 order moments. The method of parameter estimation first searches the global minimum on the larger scale, and then searches the global minimum on the smaller scale in order to avoid local minima.

Table 4. The amplitude distribution model fitting error (10^{-4})

		HH	HV	VH	VV
Data1	Rayleigh	586.3128	488.086	476.8576	404.212
	Weibull	66.6415	63.537	60.5631	45.3586
	K	82.7326	41.7739	40.1365	13.8967
	LN	33.5027	23.3846	23.7031	33.7268
	GK	27.8506	34.5025	35.6043	32.6617
	GK-LNT	**5.7927**	**3.9076**	**3.6483**	**1.3127**
Data2	Rayleigh	534.9003	231.5132	158.3669	1289.728
	Weibull	151.688	65.0759	32.7429	131.8617
	K	68.6623	14.7546	12.8744	58.7285
	LN	**9.6902**	**12.7316**	7.1948	56.5969
	GK	171.2061	185.6314	142.9841	168.5639
	GK-LNT	19.9097	15.5561	**4.2944**	**1.6264**
Data3	Rayleigh	76.9432	6.8683	32.184	107.0863
	Weibull	24.6398	2.271	31.5489	45.0309
	K	**9.1429**	103.5674	266.7979	107.7286
	LN	10.0083	17.5527	57.7872	47.825
	GK	109.3688	39.1588	36.3378	102.5827
	GK-LNT	11.4641	**0.83763**	**29.6289**	**34.6412**

Table 4 gives the fitting error of the amplitude distribution model of the clutter data. The fitting error definition is shown in the formula (3), which represents the mean square error of PDF. The least mean square error is considered as the optimal amplitude distribution model. From table 4, it can be seen that, in most cases, the GK-LNT model is more appropriate, and it is appropriate to use K or lognormal distribution in a few cases. It should be noted that, since the highly complex nature of sea clutter, the validity of the model can only be obtained through statistical analysis of clutter, but can not be obtained from the mechanism of sea clutter.

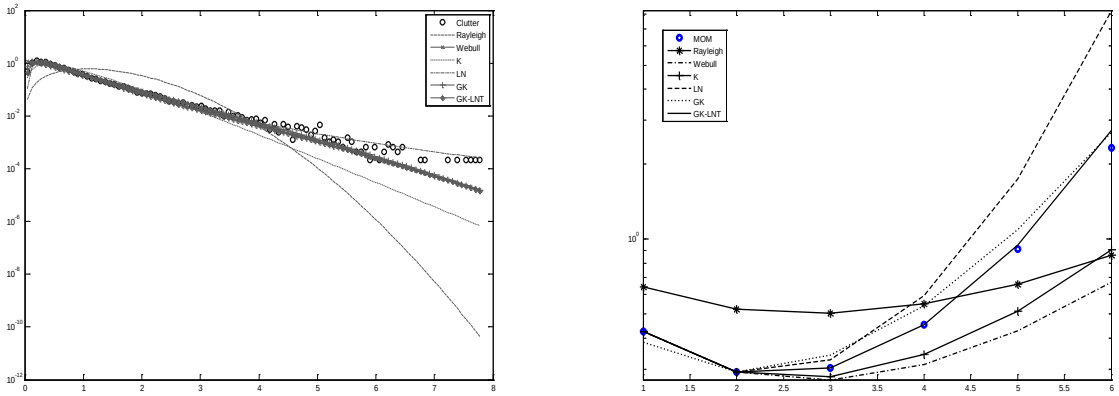

(a) Clutter amplitude PDF fitting effect (b) Estimation of the order moment of the clutter magnitude

Figure 2. The magnitude of the statistical distribution of the clutter

Figure 2 shows the fitting effect of the amplitude distribution of Data2 in VV mode. From Figure 2 (a), it can be seen that the tail of the Rayleigh distribution is the lowest, and it is not able to describe the complex amplitude distribution of the "thick tail" effect. From the actual data estimation, the "thick tail" effect is obvious, which shows that the probability of the large value of

the clutter is increased. Figure 2 (b) gives the estimation effect of the 1~6 order moment, and obviously the estimation effect of GK-LNT is the best.

PDF analysis of texture component.

The texture component in the composite Gauss model contains the full information of the non-Gaussian of the clutter. The inverse Gamma distribution is usually used as the PDF model of texture component[8]. The inverse Gamma distribution is a conjugate prior distribution of the texture components of the composite Gauss model, and the parameters of the model are of important significance for the detection of radar target[9]. The inverse Gamma distribution can be expressed as:

$$\gamma^{-1}{}_{\alpha,\beta}(\tau)=\frac{\beta^{\alpha}}{\Gamma(\alpha)}\left(\frac{1}{\tau}\right)^{\alpha+1}\exp\left(-\frac{\beta}{\tau}\right) \tag{15}$$

By using the similar method above, the texture component of the clutter is firstly extracted, or by use of the method given in reference [8], the parameters of the inverse Gamma distribution are obtained, as shown in Table 5. $k\tau\sim\gamma^{-1}(\alpha,k\beta)$, so only the shape parameters of the inverse Gamma distribution are concerned.

Table 5. Inverse Gamma distribution parameters of texture component α

	HH	HV	VH	VV
Data1	0.33949	0.37892	0.36194	0.57644
Data2	0.54236	1.3738	1.0888	0.83988
Data3	6.3728	19.2061	19.0997	13.3113

The larger shape parameters of the inverse Gamma distribution are, the sharper shape of PDF is. In the BORD detector[9], the inverse Gamma shape parameter is assumed, and the PDF of the inverse Gamma distribution is flat. As can be seen from Table 5, the shape parameters increase with improving resolution, and the shape parameters of the cross polarization are greater than Co-polar shape parameters, and the difference increases with improving resolution. This shows that the BORD can only be suitable for the low resolution clutter environment, and the increasing resolution can lead to the increase of the inverse Gamma distribution parameters, which can reduce the detection performance of BORD. So the reasonable estimation of the parameters of the inverse Gamma distribution is helpful to improve the signal detection capability in the high resolution radar clutter.

Non-Gaussian analysis of clutter in the frequency domain.

The power time-frequency distribution of the clutter can be obtained by using the short-time Fourier transform. For Gauss noise, the distribution of each Dopper frequency in the time-frequency chart satisfies the exponential distribution. So non-Gaussian can be described by the normalized second intensity moment (NSIM) [1]. For exponential distributions, the NSIM equals 2. And non-Gaussian can be judged from the size of NSIM. In this paper, the short time Fourier transform of 1024 points is used, and the results as shown in Figure 3.

Figure 3 shows the NSIM and the corresponding average power spectrum. As is shown in figure 3, the region of the clutter power spectrum is significantly non-Gaussian, while main noise is receiver noise outside the region of the clutter power spectrum, so it is Gauss, and NSIM is about 2. In the region of the clutter power spectrum, the change of Gaussian with the frequency is not uniform. The non-Gaussian is more obvious in the edge of the region of the clutter power spectrum. Secondly, the support region of the power spectrum is about 0~200Hz, and the supporting region of the NSIM is about -100~300Hz, that is, the non-Gaussian of the clutter is not restricted by the clutter power.

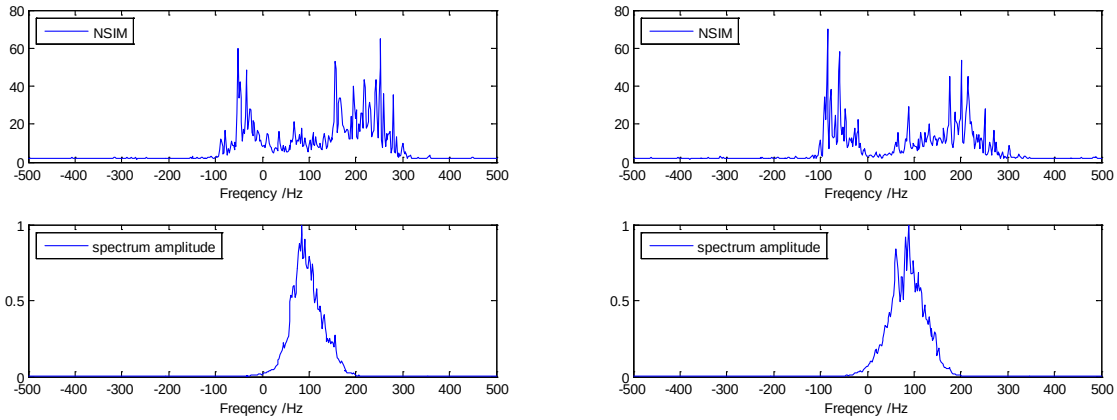

(a) Data1.HH mode (b)Data1.VV mode

Figure 3. NSIM and average power spectrum of clutter

The non-stationarity and non-homogeneity of sea clutter

The conclusion of the previous discussion is based on the average of the time, and the clutter data is analyzed about a certain range unit. The center frequency and instantaneous bandwidth of the clutter can be calculated by use of the following formula [10].

$$f_c = \frac{\int fS(f)\mathrm{d}f}{\int S(f)\mathrm{d}f} \tag{16}$$

$$B_w = \sqrt{\frac{\int (f - f_c)^2 S(f)\mathrm{d}f}{\int S(f)\mathrm{d}f}} \tag{17}$$

Using the short time Fourier transform, the center frequency and bandwidth of each window are obtained, and the results in Figure 4 can be obtained. Data2 is used in HH mode, and the center frequency and bandwidth are approximately inversely proportional. The bandwidth decreases with the increase of the center frequency, while the bandwidth will increase with the reducing of center frequency. The dynamic range of instantaneous frequency and instantaneous bandwidth is more than 100Hz. The quality factor is defined as the ratio of the bandwidth to the central frequency, as shown in Figure 4, mainly between 2~6. Similarly, the relationship between the central frequency and the bandwidth can be listed under different resolutions and different polarization combinations. The conclusion is similar to that of Table 3, and is no longer discussed. From the results of the analysis of Figure 4, the sea clutter has obvious non-stationarity.

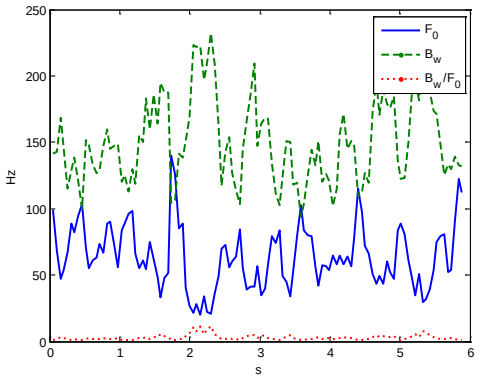

Figure 4. Non-stationarity of clutter

The statistical properties of the clutter vary with the different distance units, thus showing the non-homogeneity. In this paper, the shape parameters of the inverse Gamma distribution of the clutter texture components are studied with the distance element.

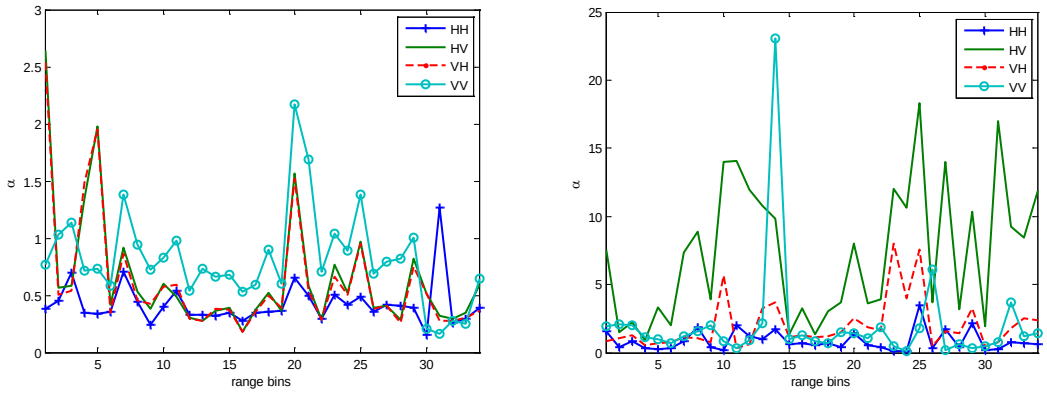

(a) Data3 (b) Data4

Figure 5. The shape parameters of inverse Gamma distribution of clutter texture components with distance

Figure 5 shows the relationship between the shape parameters of the inverse Gamma distribution of the clutter texture components and the distance variation. Comparing the clutter data under two resolutions, the range of the shape parameters obviously increases when the resolution is improved, That is say, the change of texture component distribution parameters is more obvious.

Secondly, the shape parameters of the second HH polarization condition are usually smaller, while the shape parameters of the VV polarization condition are larger. The results also show that the shape parameters of the two cross polarization under the low resolution are almost the same, but it is not the case when resolution is raised. Therefore, for the low resolution radar clutter, the homogeneity is easy to reach, but when the resolution is raised, the homogeneity can not be achieved.

Figure 6 shows the spatial correlation of texture components in 6 different resolutions of HH polarization mode, It can be seen that, the correlation coefficient of the texture components of the adjacent distance element is 0.2, but the correlation coefficient of the texture components of the non-adjacent distance element is below 0.1. This shows that, the texture component has spatial correlation, and it is not completely related, nor is it completely irrelevant.

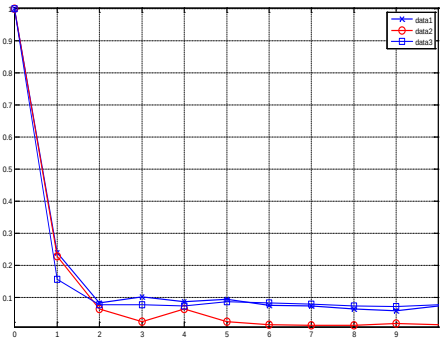

Figure 6. Spatial correlation coefficient of clutter texture components in HH polarization mode

Conclusion

In the process of radar signal detection, the statistical properties of clutter and its change with time and space are important for the design and performance evaluation of radar signal detection algorithm. In this paper, we analyze the non-Gaussian, non-stationarity and non-homogeneity of the X band sea clutter data with different range resolutions and different polarization combinations. The sea clutter of the X band can be described by the compound Gauss model. Firstly, the texture components extraction algorithm and the power spectrum analysis of the clutter is given. In analyzing process of non-Gaussian, the fitting degree of some non-Gaussian clutter model is discussed, and the conclusion is that, fitting effect of the generalized K distribution model based on the texture of lognormal distribution is the best. The parameter estimation of the inverse Gamma

distribution of texture components and the non-Gaussian in frequency domain are also discussed. Finally, the variation of statistical properties of sea clutter with distance and time is discussed. Above results show that, the sea clutter has obvious non-Gaussian, non-stationarity and non-homogeneity.

References

[1] K.D.Ward, R.J.A.Tough, S.Watts, Sea clutter: Scattering, the K distribution and radar performance, IET Radar, sonar, navigation and avionics series 20, 2006

[2] E.Conte, G.Ricci, Performance prediction in Compound-Gaussian clutter, IEEE transaction on AES, Vol.30(2):611-616,1994

[3] E.J.Kelly, An Adaptive Detection Algorithm, IEEE transactions on AES, Vol.20(1):115-127,1986

[4] C.D.Richmond, Performance of a Class of Adaptive Detection Algorithms in Nonhomogeneous Environments, IEEE transaction on SP, Vol.48(5):1248-1262,2000

[5] E.Conte, A.D.Maio, C.Galdi, Statistical analysis of real clutter at different range resolution, IEEE transaction on AES, Vol.40(3):903-918, 2004

[6] E.Conte, M.D.Bisceglie, C.Galdi, G.Ricci, A procedure for measuring the coherence length of the sea clutter, IEEE transaction on SP, Vol.46(4):836-841,1997

[7] J.C.Moya, J.G.Menoyo, A.B.D.Campo, A.A.Lopez, Statistical analysis of a high resolution sea clutter database, IEEE transactions on GRS, Vol.48(4):2024-2037, 2010

[8] A.Balleri, A.Nehorai, J.Wang, Maximum likelihood estimation for compound Gaussian clutter with inverse Gamma texture, IEEE transaction on AES, Vol.43(2):775-780,2007

[9] E.Jay, J.P.Ovarlez, D.Declercq, P.Duvaut, BORD: Bayesian optimum radar detector, Signal Processing, Vol.83(6):1151-1162, 2003

[10] M.Greco, F.Bordoni, F.Gini, X-band sea clutter nonstationarity: influence of long wave, IEEE J. OE, Vol.29(2):269-283,2004